Flexibility of Prolyl Oligopeptidase: Molecular Dynamics and Molecular Framework Analysis of the Potential Substrate Pathways

Monika Fuxreiter, Csaba Magyar, Tünde Juhász, Zoltán Szeltner, László Polgár,* and István Simon*
Institute of Enzymology, Biological Research Center, Hungarian Academy of Sciences, Budapest, Hungary

ABSTRACT **The flexibility of prolyl oligopeptidase has been investigated using molecular dynamics (MD) and molecular framework approaches to delineate the route of the substrate to the active site. The selectivity of the enzyme is mediated by a seven-bladed β-propeller that in the crystal structure does not indicate the possible passage for the substrate to the catalytic center. Its open topology however, could allow the blades to move apart and let the substrate into the large central cavity. Flexibility analysis of prolyl oligopeptidase structure using the FIRST (Floppy Inclusion and Rigid Substructure Topology) approach and the atomic fluctuations derived from MD simulations demonstrated the rigidity of the propeller domain, which does not permit the substrate to approach the active site through this domain. Instead, a smaller tunnel at the inter-domain region comprising the highly flexible N-terminal segment of the peptidase domain and a facing hydrophilic loop from the propeller (residues 192–205) was identified by cross-correlation analysis and essential dynamics as the only potential pathway for the substrate. The functional importance of the flexible loop has been also verified by kinetic analysis of the enzyme with a split loop. Catalytic effect of engineered disulfide bridges was rationalized by characterizing the concerted motions of the two domains. Proteins 2005;60:504–512.**

INTRODUCTION

There is a relatively new group of serine peptidases, unrelated to the well-known trypsin and subtilisin families. This group, the prolyl oligopeptidase family, includes enzymes of different specificities, like the prolyl oligopeptidase itself, dipeptidyl-peptidase IV, acylaminoacyl-peptidase, and oligopeptidase B.[1–3] They are in common in selecting and cleaving substrates of no longer than about 30 amino acid residues in length. Prolyl oligopeptidase (EC 3.4.21.26) is implicated in the metabolism of peptide hormones and neuropeptides.[4–8] Since specific inhibitors relieve scopolamine-induced amnesia,[9–12] the enzyme is of pharmaceutical interest. The activity of prolyl oligopeptidase has also been connected with depression[13–15] and blood pressure regulation.[16]

The crystal structure determination of prolyl oligopeptidase has revealed that the peptidase domain of the enzyme displays an α/β hydrolase fold, and that its catalytic triad (Ser 554, His 680, Asp 641) is covered by the central tunnel of an unusual β-propeller[17] [Fig. 1(A)]. The β-Propellers contain four- to eightfold repeats of four-stranded antiparallel β-sheets, which are twisted and radially arranged around a central tunnel.[18–20] Nearly all of the known propeller proteins have evolved ways to close the circle (linked by "Velcro") between their first and last blades. For example, in the β-subunit of G proteins six of the seven blades of the propeller domain are built up regularly, forming four-stranded antiparallel β-sheets. The six blades are joined in succession around the central pseudo-7-fold axis. In blade 7, however, the ring closure is achieved by forming the four antiparallel β-strands from both termini of the propeller domain. The N-terminus of the propeller domain provides the outermost strand, which is connected via main-chain hydrogen bonds to the three antiparallel β-strands from the C-terminus of the propeller. While the six-, seven-, and eight-bladed propellers snap the "Velcro" in a similar way, the smaller four-bladed forms a disulfide bond between the first and last blades.

The seven-bladed β-propeller of prolyl oligopeptidase is different from the above mentioned structures. The circular structure is not stabilized by "Velcro" or disulfide bond [Fig. 1(B)]; primarily hydrophobic interactions connect the first and last blades that might allow the propeller to regulate the access of substrate to the active site. However, the diameter of the hole at the bottom of the propeller is ~ 4 Å, that is too small for the entry of the oligopeptide substrate. The crystal structure did not reveal any other opening, which would be sufficiently large for the substrate to pass through.[17] In contrast, the recently determined crystal structure of dipeptidyl peptidase IV, a member of the same enzyme family, revealed an eight-bladed propeller of open-velcro topology instead of seven-bladed, observed in prolyl oligopeptidase. In dipeptidyl peptidase IV two tunnels run to the active site: one is the central tunnel with larger hole at the distal end of the propeller than the corresponding hole in prolyl oligopepti-

Grant sponsor: Wellcome Trust; Grant number: 066099/01/Z; Grant sponsor: OTKA; Grant numbers: T046057, T34131, F046164, D38487

*Correspondence to: István Simon, Institute of Enzymology, Biological Research Center, Hungarian Academy of Sciences, H-1518 Budapest Pf.7, Hungary. E-mail: simon@enzim.hu

Received 11 November 2004; Revised 2 February 2005; Accepted 2 February 2005

Published online 21 June 2005 in Wiley InterScience (www.interscience.wiley.com). DOI: 10.1002/prot.20508

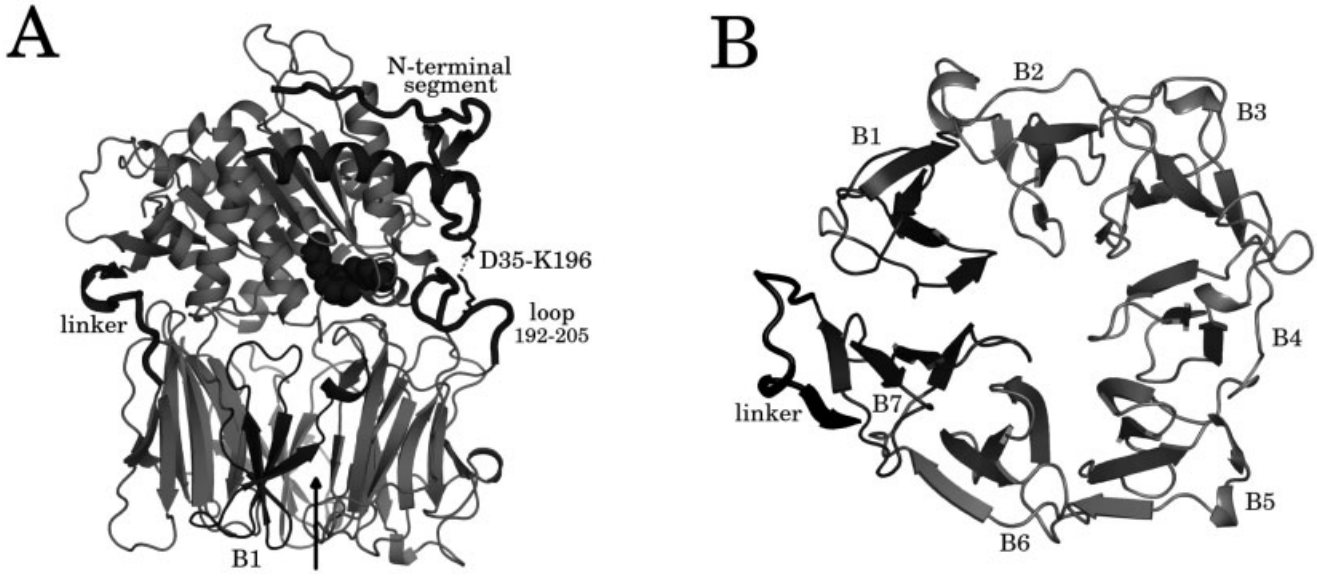

Fig. 1. Ribbon representation of the crystal structure of prolyl-oligopeptidase. PDB code number 1QFM.[17] **A:** The upper part is the peptidase domain, the lower is the propeller comprised of seven blades. The active site (Ser-554, His-680, Asp-641) is shown by space filling model. The N terminal segment, the facing hydrophilic loop (residues 192–205) and the linker between the two domains (residues 425–437) are displayed by thicker black lines. Arrow at the bottom points to the entrance of the central tunnel of the propeller, which is too small (4 Å) to allow the substrate to enter the protein. **B:** The top view of the β-propeller structure. The blades are numbered as B1–B7. Blades B1 and B7 are not linked by a "Velcro."

dase, and the other with an even larger opening is located at the side of the propeller. The size of the latter opening is more than 20 Å, suitable for the entry or the egress of a substrate without conformational changes.[21] It is also assumed that substrates approach the buried active site through the central tunnel, while products leave the cavity through the separate side exit[22] or use the opposite direction.[23]

Because of the lack of an apparent entrance in prolyl oligopeptidase, substantial main-chain conformational changes are expected to accompany substrate binding involving highly flexible protein regions. We have previously shown that limiting the motions either between the blades or between the two domains by engineering disulfide bridges between them can block the enzymatic activity by limiting the access to the active site.[24] These results suggested that concerted movements of the propeller and the peptidase domains are required to open up a sufficiently large entrance for the substrate.

To locate the possible passage of the substrate to the active site, in this work we characterized the flexibility of prolyl oligopeptidase using molecular dynamics and molecular framework approaches. Two possibilities for the substrate entry were considered: (1) the first and the seventh blades move apart to enlarge the hole at the distal end of the propeller, and (2) the two domains separate and allow the substrate to approach the active site. For the prolyl oligopeptidase from the thermophile *Pyrococcus furiosus*, which is a more stable and smaller enzyme, it was suggested that the substrate may approach the active site between the two domains.[25] In this work most part of the propeller, with the exception of the loops connecting the β-strands, has been identified as a rigid cluster, in agreement with the small thermal motions derived from the atomic fluctuations of the MD simulation. Cross-correlation analysis demonstrated that the motions of the first and seventh blades are correlated, weakening the hypothesis that the noncovalent links of the propeller would allow its opening. Instead, the N-terminal segment and the facing hydrophilic loop of the propeller domain move in anti-correlated fashion that can result in the enlargement of a small cavity located between the two domains. The animation of the concerted motions of the molecule to which the N-terminal segment provides dominant contribution confirms the prediction that the small tunnel can serve for substrate entry. The impact of this cavity on substrate binding has also been probed by kinetic studies of the enzyme modified at the hydrophilic loop.

MATERIALS AND METHODS

Flexibility Analysis

Analysis of the molecular topography was done by the molecular framework approach FIRST (Floppy Inclusion and Rigid Substructure Topology).[26] In the FIRST algorithm the protein molecule is represented as a bond-bending network defined by the covalent and hydrogen bonds as well as salt bridges of the crystal structure. The overconstrained and underconstrained protein segments are determined based on the degrees of freedom of this network. A substructure is considered overconstrained (i.e., rigid), if contains more cross-linking bonds than necessary to keep the region rigid, while underconstrained (i.e., flexible), if less such cross-linking occurs. As a measure of flexibility the flexibility index used that is defined based on the number of extra bonds or remaining degrees of freedom as follows: (1) $f_i = F_k/H_k$, where F_k is the number of floppy modes and H_k is the number of rotatable bonds (hinge joints) within the *k* underconstrained region

of the protein; (2) $f_i = -R_j/C_j$, where R_j is the number of redundant constraints and C_j is the number of central force bonds (nearest neighbor contacts) in a j overconstrained region of the protein; (3) 0 in isostatically rigid region, which contains no redundant constraints. Clusters or a set of clusters with few independent degrees of freedom are considered as collective motions. The FIRST analysis was found to predict flexibility changes upon protein–substrate binding using a static structure in good agreement with the molecular dynamics results.[27] Therefore, we have applied both methods to study flexibility properties of prolyl-oligopeptidase.

The network properties depend on the energetics of hydrogen bonds considered. In this work a −1.5 kcal/mol threshold was used. Rigid cluster decomposition, flexibility index calculations, and collective motion predictions were done by the program FIRST (http://firstweb.asu.edu).

Molecular Dynamics Calculations

The starting model of prolyl oligopeptidase has been derived from the 1.4-Å resolution crystal structure of the free protein (PDB code: 1QFM).[17] All heteroatoms (glycerol, 1-hydroxy-1thio-glycerol) have been removed and cysteine derivatives (cysteine-S-dioxide and S-oxy cysteine) were replaced by cysteines. The model was completed with hydrogens and 21 counterions were placed around the ionizable side chains located on the surface to achieve electroneutrality. The protein has been immersed in a rectangular cell of waters with 103 Å × 78.6 Å × 80.7 Å dimensions. The protein atoms were represented by the AMBER94 force field,[28] while for water the TIP3P model was used.[29] The system was subjected to an extensive pre-equilibration process, in which the water atoms and counterions were relaxed in course of a minimization followed by a 100-psec molecular dynamics (MD) at 600 K to let more waters enter the protein. Then a 3-psec MD run using isotherm-isobar ensemble has been applied to adjust the box dimensions. Subsequently the protein atoms were minimized for 22,000 steps until the maximum gradient dropped below 0.5 kcal/mol Å. A molecular dynamics simulation with a step size of 2 fsec was conducted at 300 K at constant pressure. The cutoff for nonbonded interactions was set to 9 Å. Snapshots were collected at 0.1 psec intervals during a 1 nsec production run. The simulation was performed using the Sander module of the AMBER program version 7.0.[30]

Root-mean-square amplitude of motion of C_α atoms around their equilibrium positions were computed as

$$\langle u_i^2 \rangle^{1/2} = \left[\frac{1}{N} \sum_{j=1}^{N} \Delta x_i(t_j)^2 \right]^{1/2} \quad (1)$$

where N is the number of configurations and Δx_i is the deviation of the atom i from its mean position during t_j interval of the equilibrium period.

Essential Dynamics

The protein flexibility can be represented by the atomic fluctuations if a harmonic approximation is used.[31] From the atomic fluctuations the covariance matrix (**C**) can be built as:

$$C'_{ij} = \langle \Delta x_i \Delta x_j \rangle \quad (2)$$

where Δx_i and Δx_j are deviations with respect to the average coordinates of atoms i and j, and $\langle\ \rangle$ represents ensemble average at a temperature T. The overall translational and rotational degrees of freedom were removed by superimposing the configurations collected during the production run onto each other. Since we assume, that the substrate binding involves major backbone changes, only C_α atoms are used for constructing the covariance matrix.[32] The diagonal elements of **C** represent the mean-square fluctuations around a given Cartesian coordinate. The off-diagonal elements give the equal-time cross correlation function between a pair of coordinates.

In the essential dynamics (ED) method the eigenvalues and eigenvectors of the covariance matrix are determined by diagonalization.[33] The eigenvectors describe the direction of the concerted motions of the atoms, whereas eigenvalues represent the mean square fluctuations of the total displacements along these directions.

The correlation of the atomic motions is given by the equal-time cross correlation function, which is computed from normalized displacement vectors as:[34]

$$C_{ij} = D^T C_{ij} D \quad (3)$$

where C_{ij} is often given as $C_{ij} = \langle \Delta r_i \Delta r_j \rangle$ and Δr_i is the displacement vector for atom i. The diagonal elements of C'_{ij} are equal to 1. The off-diagonal elements vary between +1, representing fully correlated motion and −1 representing anti-correlated movement between a pair of atoms. Atoms, the motion of which is not coupled have cross-correlation values around 0.

Tryptic Digestion of Prolyl Oligopeptidase and Isolation of the Nicked Enzyme

Prolyl oligopeptidase from porcine brain and its truncated variants were expressed in *Escherichia coli* JM105 cells and purified as described previously.[35] The enzyme (0.46 mg/mL) was digested with trypsin (0.007 mg/mL) in 6.6 mL 0.05-M Hepes buffer (pH 8.0), containing 1 mM $CaCl_2$ at 25°C for 45 min. The reaction was stopped by the addition of 1 mM benzamidine, 5 mM DTE, and 2 mM EDTA, and then the pH was adjusted to 6.5 with 0.2 M NaH_2PO_4. The resulting solution was concentrated to 2 mL by centrifugation using an ultrafiltration device (Millipore, Amicon Ultra MWCO 30,000). The concentrate applied to a Mono Q HR 10/10 FPLC column and eluted with NaCl gradient using 20 mM phosphate buffer (pH 6.5), containing 1 mM EDTA and DTE (solvent A) and 0.5 M NaCl in the same buffer (solvent B). The gradient was developed between 18–40%, during four column volumes. The fractions were analyzed by SDS PAGE, and the pure fractions containing the nicked prolyl oligopeptidase (1.1 mg) were combined. The trypsin, the native prolyl oligopeptidase and the nicked enzyme were eluted at 18, 26–28, 29–32% solvent B, respectively.

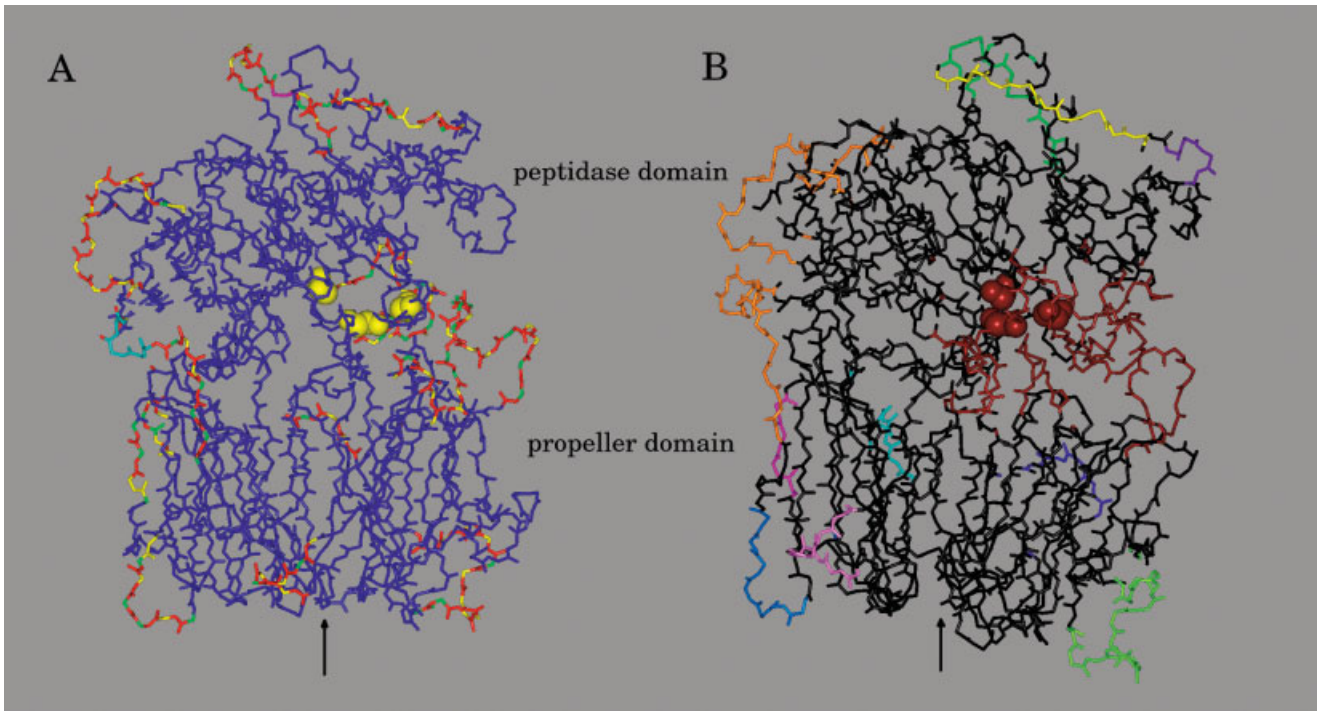

Fig. 2. **A:** Rigid cluster analysis of the crystal structure of prolyl endopeptidase. Cyan and dark blue colors correspond to rigid regions with negative flexibility indexes. Largest rigid clusters are displayed in dark blue. Flexible residues are displayed in yellow, orange, and red in the order of the increased flexibility. The active site is shown by space filling model. **B:** Collective motions in prolyl oligopeptidase. Residues belong to the same cluster are displayed by the same color. The interdomain region involving the N-terminal segment, the facing loop (residues 192–205) and the active site are colored by dark red. Rigid clusters are shown by black.

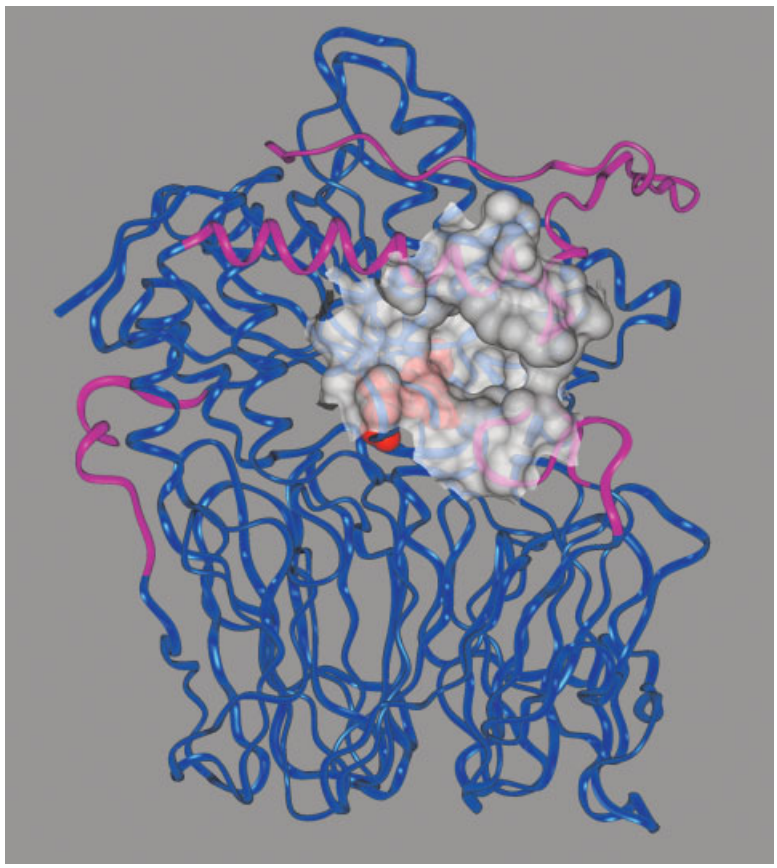

Fig. 5. Surface representation of the small cavity (invagination) that mediates between the active site and the solution. The cavity displayed in white comprises the residues 31–35, 39, 40, 43 of the N-terminal segment; facing this segment are located the residues 196, 200–202 of the hydrophilic loop and the residues 637–641, 645–647, 650, 674 from the C-terminal region. The functionally important segments are shown in magenta. The active site, which is presented by space filling model in white appears through the cavity.

Kinetics

The reaction of prolyl oligopeptidase with Z-Gly-Pro-Nap (Bachem Ltd., Bubendorf, Switzerland) was measured fluorometrically, using a Cary Eclipse fluorescence spectrophotometer equipped with a Peltier four-position multicell holder accessory and a temperature controller. The excitation and emission wavelengths were 340 and 410 nm, respectively.

The pseudo-first-order rate constants were measured at substrate concentrations lower than 0.1 K_m and were calculated by nonlinear regression data analysis, using the GraFit software.[36] The specificity rate constants (k_{cat}/K_m) were obtained by dividing the pseudo-first-order rate constant by the total enzyme concentration in the reaction mixture.

Thermodynamic Parameters

The temperature dependence of k_{cat}/K_m was determined at protein concentrations of 0.45–2.0, at temperature 5–40°C in standard buffer, containing 1 μM BSA. The thermodynamic parameters were calculated from Eyring plots (Equation 4), where k is the rate constant, R is the gas constant (8.314 J/mol.K), T is the absolute temperature, N_A is the Avogadro number (6.022×10^{23}/mol), h is the Planck constant (6.626×10^{-34} J.sec), the enthalpy of activation $\Delta H^* = -(\text{slope}) \times 8.3\ 14$ J/mol, the entropy of activation $\Delta S^* = (\text{intercept} - 23.76) \times 8.314$ J/mol.K. The free energy of activation, ΔG^*, was calculated from Equation 5.

$$\ln(k/\mathrm{T}) = \ln(R/N_A h) + \Delta S^*/R - \Delta H^*/R\mathrm{T} \quad (4)$$

$$\Delta G^{*\prime} = \Delta H^* - \mathrm{T}\Delta S^* \quad (5)$$

RESULTS

Rigid Clusters

Rigid-cluster decomposition revealed two main rigid regions in prolyl oligopeptidase: one includes the β-strands of the propeller, the other comprises the central part of the peptidase domain. The rigidity of the propeller in prolyl-oligopeptidase in common with other β-propeller structures[18,19] illustrates that the overall flexibility of this structural motif is not determined by its closed or open topology; the cluster of hydrophobic interactions serves as a powerful structure stabilizing factor. The local flexibility characteristics of prolyl-oligopeptidase are displayed in Figure 2(A). As indicated by the rigid cluster decomposition, the two domains are highly overconstrained (colored by dark blue) with the exception of the loops at the surface and at the inter-domain region. Rigidity of the two domains indicates that substrate transport through either of them is quite unlikely. Underconstrained regions (colored by red) possess less constraints than to keep them rigid, hence are likely candidates for large conformational displacements. These flexible regions include loops between the β-strands as well as the hinge (residues 424–432) that links the two domains. The largest flexible segment is located opposite to the hinge, comprises residues 192–205 of the propeller domain. This loop faces another loop from the peptidase domain (residues 578–594) that shields the active site. Flexibility of these loops suggests that substrate passage is facilitated between the two domains. Indeed, engineering a disulfide bond in this region between residues 255–597 blocks the access to the active site.[24]

Clusters with correlated motions defined based on the bond-bending network of the protein are represented as color-coded in Figure 2(B). Analysis of the collective motions reveals cooperation between the two domains that involves the long flexible loop of the propeller domain (residues 192–205) and the active-site residues of the peptidase domain suggesting the functional importance of this loop in substrate binding.

Molecular Dynamics

The absence of an opening with appropriate size in the crystal structure of prolyl oligopeptidase indicates that considerable conformational changes are required for the substrate entry that involves flexible protein segments. The flexibility of each residue was characterized by the fluctuation around their average positions in the equilibrium period of the MD simulation. The B factors computed from the root-mean-square displacements as $B = 8/3\pi^2 u^2$, where u is the mean displacement of the atom, were compared to the thermal fluctuations in the crystal structure [shown for C_α atoms in Fig. 3(A)]. As expected, fluctuations in solution are generally larger than in the crystal structure; with average B factors of 15.0 Å^2 versus 11.2 Å^2, respectively. Some segments, like the hinge region (residues 424–432) however, turned out to be less flexible in the simulation reflecting that domain motions are constrained in the crystal structure. While the crystal structure shows similar flexibility of the two domains, they exhibit different dynamics in solution; fluctuations of the propeller domain become larger than those of the peptidase domain with the exception of the N-terminal segment. This implicates the role of the propeller domain in regulation of substrate binding.

The most pronounced difference in flexibility between the crystal and the simulated structure can be observed at the N terminal region including residues 10–25 and 30–38. These residues are not involved in crystal contacts; therefore the increased fluctuations in solution are due to their intrinsic flexibility and not the consequence of removing the crystallographic constraints. The facing hydrophilic loop in the propeller region (residues 192–205) that was identified as the longest flexible segment by the FIRST analysis has relatively high B factors (25 Å^2) in the crystal structure, which almost remain unchanged in the simulation. In contrast, fluctuation of the surface loops increase substantially in the simulation, including the loop of the peptidase domain (residues 581–608) that faces the hydrophilic loop (residues 192–205) of the propeller region. Separation of these two loops could open an entrance between the two domains that can facilitate the substrate access to the active site. Insertion of a covalent link between them (C255–T597C) can inhibit such separa-

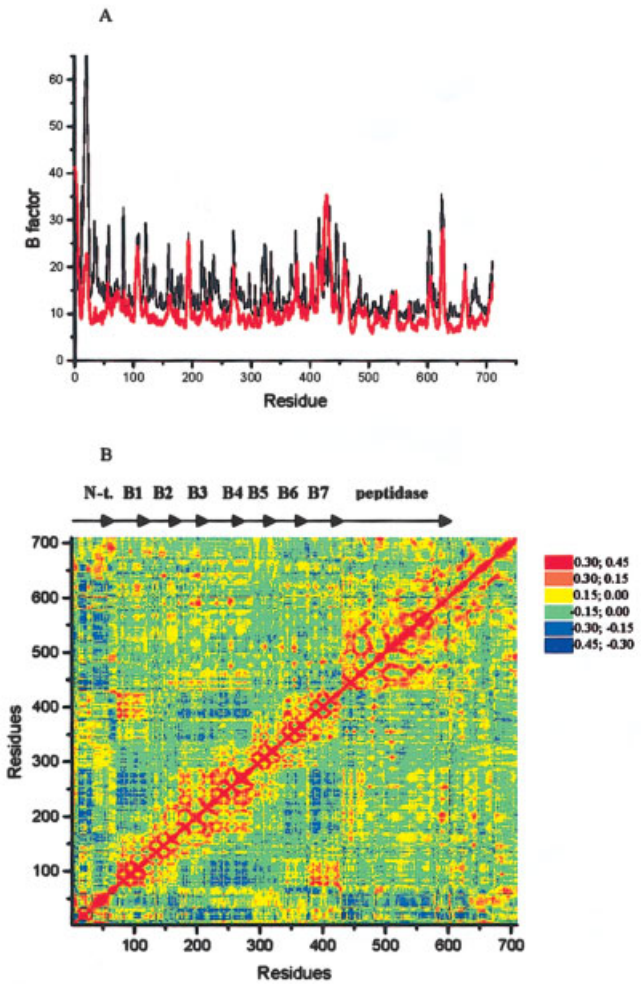

Fig. 3. **A:** Comparison of the B factors of the C_α atoms computed from the thermal fluctuations during the 2.6–3.6 nsec period of the MD simulation (thin black line) with those observed in the crystal structure (bold red line). **B:** Cross-correlation map of C_α fluctuations. Color scale can be found at the right side of the figure. Residues with correlated motions, such as the B1 and B7, B3 and B4 are displayed in red and orange. Negative correlations corresponding to movements to opposite directions, are colored by blue. Such anti-correlation is observed between B1 and B4 of the propeller; the N-terminal segment and B4 blade, the loop involving residues 192–205, the linker region and a part of the peptidase domain that includes the active site Ser-554 and Asp-641. Cyan and green areas show residues with weakly coupled motions. The position of each blade is shown at the top of the figure.

tion and interfere with substrate binding, as it has been shown experimentally.[24]

Highly flexible segments however, can be found in the neighborhood of all engineered disulfide bridge positions suggesting that their suppressing effect is related to the perturbation of the concerted movement of the molecule that is essential for the substrate pathway rather than to blocking the actual entrance.

Cross-Correlations

Opening and closing motions relating to the substrate transport can be expected at regions with anti-correlated motions that can be identified by the cross-correlation functions of the atomic fluctuations. The cross-correlations of the C_α atomic displacements are illustrated in Figure 3(B).

As expected, the correlations between the residue movements within each blade are strong, presented by orange-red squares around the diagonal of the map. A considerable correlation is also observed between the motions of blades B3 and B4, B6, and B7 as well as B1 and B7. A weaker coupling is found between B5 and B6. The correlation between the movements of B1 and B7 excludes the possibility that the separation of these two not covalently connected blades allow the substrate to enter the protein. Movements of B1 and B4 are anti-correlated, just like those of B3-B4 with B6-B7 (in particular with B7). Movements of the blades located at opposite sides of the propeller into opposite directions indicate that this domain can undergo an opening-closing motion that is perpendicular to the axis of the propeller (see below). The expansion of the propeller, however, would require that the other pair of blades (B2 and B5) also move into opposite directions. Such anti-correlation, however, was not shown by the cross-correlation functions demonstrating that opening the entrance of the propeller is unlikely in the free protein, due to the network of extensive hydrophobic contacts between the blades.

Considerable anti-correlation is found between the movement of the N-terminal segment (residues 10–60) and several other parts of the molecule; the B3 and B4 of the propeller, the hinge region that links the two domains and two segments (residues 525–575 and 615–660) that contain the catalytic Ser-554 and Asp-641. These observations illustrate that coupling between the active site and the propeller domain is essential for substrate binding in prolyl oligopeptidase.[24]

Motions of the peptidase domain with the exception of the N-terminal region (residues 10–60) are self-correlated. Since the fluctuations of these residues are small, this part of the molecule behaves as a rigid cluster as it has been predicted by the FIRST analysis. A slight correlation between the segment (residues 433–470) following the inter-domain linker and the B3-B4 blades of the propeller was found, supporting the hypothesis that concerted movements are required for proper functioning of prolyl oligopeptidase.

Essential Dynamics

To characterize the direction of the concerted motions of the atoms, we have determined the eigenvectors of the covariance matrix constructed from the fluctuations of the C_α atoms during the 2.6–3.6-nsec period of the trajectory. The eigenvalues that represent the mean square fluctuations of the total displacements along these directions covered the frequency range of 22.6–7121 cm^{-1}.

The low-frequency modes between 22.6–199.7 cm^{-1} were considered functionally relevant[37] and the belonging 49 eigenvectors were visualized. The two domains exhibit concerted motion: they rotate to opposite directions perpendicular to the axis of the propeller. Due to its enhanced flexibility, the N-terminal domain (ca. residues 10–40)

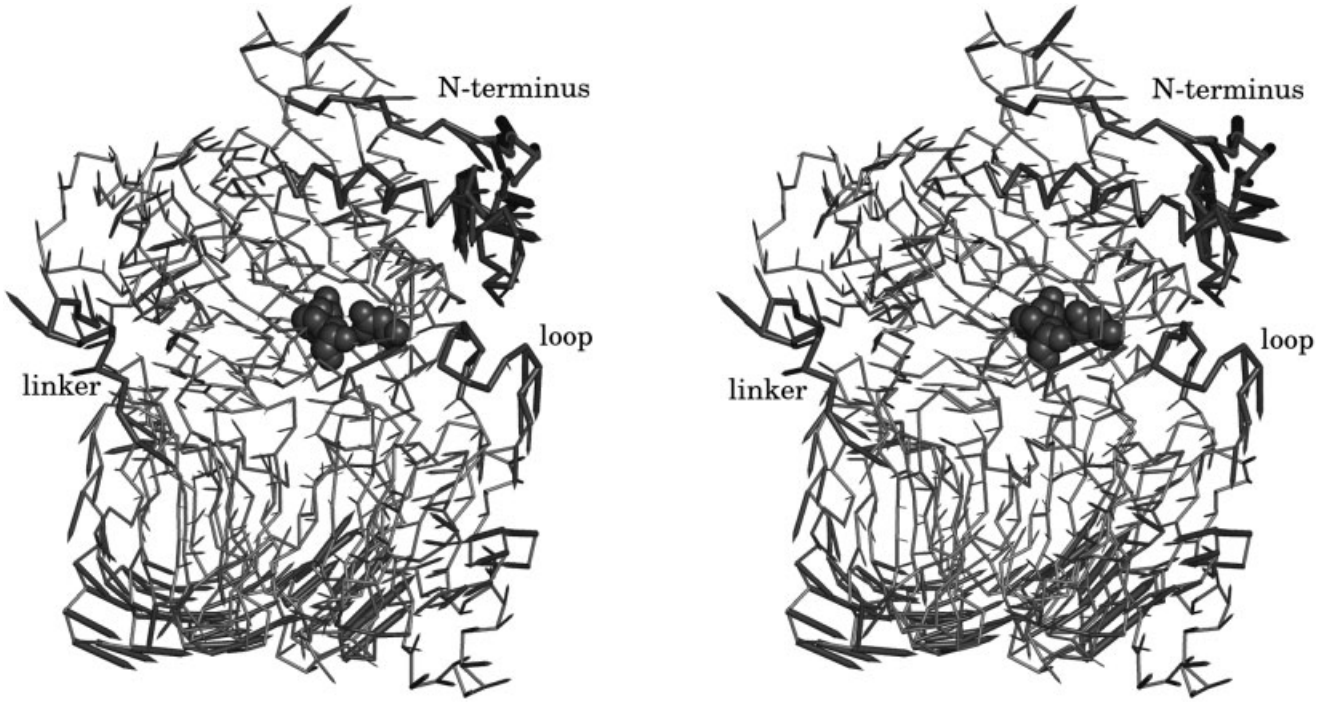

Fig. 4. Stereodiagram of the eigenvectors in mode 7 (ν = 76.1 cm^{-1}) representing the directions of the concerted motions of the atoms. The magnitude of the vectors is proportional to the mean square fluctuations of the total displacements. The contribution of the N terminal segment is dominant in modes 1–7. The protease domain (upper part) and the propeller (lower part) rotate in opposite directions.

provides a major contribution to the first seven eigenvectors with largest amplitudes. This segment performs an opening movement on the top of the peptidase domain (Fig. 4). The up and down movement of the N-terminal loop is coupled to the rotation of the two domains that can facilitate the separation of the propeller and peptidase segments. Indeed, the distance between the two domains increases from 6.8 Å to 9.3 Å (measured between Pro34 and Thr200) during the MD simulation. In contrast, no eigenvectors contributing to the opening of the propeller entrance have been observed. Thus directions of the concerted motions indicate that the substrate is more likely to approach the active site between the two domains rather than through the propeller.

To delineate the possible pathway of the substrate, we searched for openings that could uncover the active site and make it accessible from the surrounding solution. To this end we constructed the linear combination of eigenvectors that contain large contributions by residues with anti-correlated motions, weighted all vectors by the corresponding eigenvalues and generated 10 snapshots along the direction of the combined eigenvectors. The animation of the snapshots revealed the enlargement of a small cavity that unveils the active site and can guide the substrate to the catalytic center. This cavity is lined by residues 31–35, 39, 40, 43 of the N-terminal segment, residues 637–641, 645–647, 650, 674 from the C terminal region including the catalytic Asp-641 and 196, 200–202 of the flexible hydrophilic loop (Fig. 5). The volume of this invagination is 241 Å^3 in the crystal structure and increases to 670 Å^3 during the MD simulation as computed by the VOIDOO program.[38] Such enlargement corresponds to the increase of the cavity diameter by $\sim$ 2.5 Å as measured between the C_α atoms of residues 34 and 200. In contrast, the hole at the bottom of the propeller is contracted. This small cavity is conserved in the structure of prolyl oligopeptidase in complex with inhibitor (PDB code: 1QFS[17]) and also in that of the S554A mutant with substrate (PDB code: 1UOO[39]) with volumes of 253 Å^3 and 210 Å^3, respectively.

The enhanced flexibilities of the cavity forming residues, the anti-correlation between their motions and the directions of these concerted movements make this cavity as a likely candidate for substrate entry. This hypothesis has also been probed experimentally.

Cleaving the Long Loop at the Substrate Entrance

The hydrophilic loop comprising residues 192–205 that has been predicted as part of the potential entrance for the substrate, is connected to the N-terminal segment via a salt bridge between Lys196 and Asp35 (2.67 Å). This salt-bridge shown in Figure 1(A) appears to obstruct the route to the active site.

We have previously shown that prolyl oligopeptidase can be cleaved with trypsin at the single bond Lys196–Ser197 with moderate changes in the catalytic activity.[40] If the separation of Lys196 and Asp35 affects substrate binding, as it has been proposed above, increasing flexibility of this region by introducing a nick should improve K_m. To this end we have examined the pH dependence of the k_{cat}/K_m after tryptic digestion. The rate constant measured at the maximum activity was remarkably higher

TABLE I. Activation Parameters for the Reaction of Prolyl Oligopeptidase With Z-Gly-Pro-Nap

Enzyme	ΔH^* (kJ/mol)	ΔS^* (kJ/mol×K)	ΔG^* (kJ/mol)
Wild type	61.6	88.4	35.2
Nicked	66.0	114.2	32.0

with the nicked prolyl oligopeptidase (10.0 $\mu M^{-1}s^{-1}$) than with the wild type enzyme (1.75 μM^1s^1). It conforms the proposal that substrate binding is accompanied by the movement of this loop. We must note that according to the temperature scanning with DSC the cleavage of the loop did not have any significant effect on the stability of the enzyme as compared to the wild type (data not shown).

The activation enthalpy (ΔH^*) and entropy (ΔS^*) of the reaction with the nicked prolyl oligopeptidase were calculated using the linear Eyring plots for k_{cat}/K_m (Table I). The activation free energy of the nicked enzyme is lower than that of the wild type due to the entropic contribution. The almost 30% increase in ΔS^* of the nicked enzyme over the wild type suggests that it is indeed the increased structural flexibility of the loop 192–205 that facilitates the substrate access and thus improves k_{cat}/K_m.

DISCUSSION

Local flexibilities are expected to play key role in the substrate binding to prolyl oligopeptidase, since considerable conformational changes of the crystal structure are required to create sufficiently large opening for the substrate. To unravel the potential pathway through the oligopeptidase molecule toward the active site, we applied molecular framework and molecular dynamics approaches to characterize the intrinsic flexibilities of the different protein regions.

Prolyl oligopeptidase has a unique β-propeller structure lacking the Velcro closure that was proposed to allow the separation of the first and seventh blades and thereby facilitate the substrate entry. Local flexibilities by both the FIRST analysis and MD simulations unambiguously demonstrated that despite the open topology, this structural motif is rigid, similarly to other β-propeller structures. Motions of the B1 and B7 blades are correlated that prevents their separation. Cross correlation functions indicate opening-closing motions between the first and fourth blades, but not between the other pairs of blades that would be required for propeller expansion. Indeed, the size of the potential entrance at the bottom of the propeller [Fig. 1(A)] is slightly decreased during the MD simulation (by ~ 1.5 Å). We can conclude that clusters of hydrophobic interactions between the neighboring blades provide strong contacts that are difficult to break by separation of the blades during propeller expansion. They can be maintained however, by sliding the blades on each other [in parallel to the vertical axis of the molecule, Fig. 1(A)]. These motions are coupled to the motions of the peptidase domain and thus can play role in the separation of the two domains. These correlations can interfere with substrate binding that results in impaired enzymatic activity upon insertion of disulfide bridges between different blades.[24] We must note that although concerted motions can be important for the actual chemical step of the catalysis our study did not address this question.

The propeller and the peptidase domains are connected by a flexible linker. The absence of covalent contacts opposite to this hinge would allow the separation of the two domains. Both molecular framework and molecular dynamics identified several flexible segments in this region, the movement of which could make the active site accessible from solution. These segments constitute a small tunnel that involves the active-site Asp-641. Anticorrelated motions of these segments lead to the enlargement of the opening of the tunnel that can facilitate the substrate access to the catalytic center. The entrance of the tunnel has been shown to increase considerably in the MD simulation. The tunnel is formed by the N-terminal segment (residues 10–40), a facing hydrophilic loop of the propeller domain (residues 192–205) and some residues from the C terminal region (637–641, 645–647, 650, 674). The N-terminal region provides a major contribution to the largest amplitude movements of the prolyl oligopetidase molecule. The motions of this segment are coupled to those of the two domains: rotation of the peptidase and propeller domains to opposite directions lead to the raising of the N-terminal segment (Fig. 4) suggesting that the molecule will open up in this region. The functional importance of the hydrophilic loop was also examined experimentally.

In the crystal structure the potential substrate entrance is blocked by a salt bridge formed between Asp35 of the N-terminal segment and Lys196 of the facing hydrophilic loop. The flexibility of both segments allows them to break this noncovalent linkage, as it was observed in the molecular dynamics simulation. Previously trypsin has been found to cleave prolyl oligopeptidase at the single bond Lys196–Ser197[41] confirming that the salt-bridge breaks down in solution and the loop moves considerably in order that the lysine side chain be available for the specificity pocket of trypsin. Moving the loops apart can open the potential pathway for the substrate toward the active site. Increased k_{cat}/K_m of the cleaved enzyme is also consistent with these results and provides strong support for the involvement of this loop substrate passage. No other potential entry for the substrate could be located besides the small tunnel, for which the functional importance has been computationally and experimentally demonstrated.

Our results also indicate that the substrate access to the active site, which is a major regulatory mechanism of the oligopeptidase activity, is different in prolyl oligopeptidase and the related dipeptidyl peptidase IV.

ACKNOWLEDGMENTS

M.F. and Cs. M. also acknowledge the NIIF supercomputer center for computer time (project numbers 1067 and 1053). Thanks are due to Ms. I. Szamosi for excellent technical assistance. Authors are grateful to Brandon Hespenheid (Arizona State University) for useful advices on the FIRSTweb server.

REFERENCES

1. Rennex D, Hemmings BA, Hofsteenge J, Stone SR. cDNA cloning of porcine brain prolyl endopeptidase and identification of active site seryl residue. Biochemistry 1991;30:2195–2203.
2. Rawlings ND, Polgár L, Barrett AJ. A new family of serine-type peptidases related to prolyl oligopeptidase. Biochem J 1991;279: 907–908.
3. Polgár L. Prolyl oligopeptidases. Methods Enzymol 1994;244:188–200.
4. Wilk S. Prolyl endopeptidase. Life Sci 1983;33:2149–2157.
5. Mentlein R. Proline residues in the maturation and degradation of peptide hormones and neuropeptides. FEBS Lett 1988;234:251–2566.
6. Cunningham DF, O'Connor B. Proline specific peptidases. Biochim Biophys Acta 1997;1343:160–183.
7. Polgár L. The prolyl oligopeptidase family. Cell Mol Life Sci 2002;59:349–362.
8. Polgár L. Structure-function of prolyl oligopeptidase and its role in neurological disorders. Curr Med Chem—Central Nervous System Agents 2002;2:251–257.
9. Yoshimoto T, Kado K, Matsubara F, Koriyama N, Kaneto H, Tsuru D. Specific inhibitors for prolyl endopeptidase and their anti amnesic effect. J Pharmacobio-Dyn 1987;10:730–735.
10. Atack JR, Suman-Chauhan N, Dawson G, Kulagowski JJ. In vitro and in vivo inhibition of prolyl endopeptidase. Eur J Pharmacol 1991;205:147–163.
11. Miura N, Shibata S, Watanabe S. Increase in the septal vasopressin content by prolyl endopeptidase inhibitors in rats. Neurosci Lett 1995;196:128–130.
12. Portevin B, Benoist A, Remond G, Herve Y, Vincent M, Lepagnol J, De Nanteuil G. New prolyl endopeptidase inhibitors: in vitro and in vivo activities of azabicyclo[2.2.2]octane, azabicyclo-[2.2.1]heptane, and perhydroindole derivatives. J Med Chem 1996;39:2379–2391.
13. Maes M, Goossens F, Scharpe S, Meltzer HY, D'Hondt P, Cosyns P. Lower serum prolyl endopeptidase enzyme activity in major depression: further evidence that peptidases play a role in the pathophysiology of depression. Biol Psychiatry 1994;35:545–552.
14. Williams RS, Eames M, Ryves WJ, Viggars J, Harwood AJ. Loss of a prolyl oligopeptidase confers resistance to lithium by elevation of inositol (1,4,5) trisphosphate. Embo J 1999;18:2734–2745.
15. Williams RS, Cheng L, Mudge AW, Harwood AJ. A common mechanism of action for three mood-stabilizing drugs. Nature 2002;417:292–295.
16. Welches WR, Brosnihan KB, Ferrario CM. A comparison of the properties and enzymatic activities of three angiotensin processing enzymes: angiotensin converting enzyme, prolyl endopeptidase and neutral endopeptidase 24.11. Life Sci 1993;52:1461–1480.
17. Fülöp V, Böcskei Z, Polgár L. Prolyl oligopeptidase: an unusual beta-propeller domain regulates proteolysis. Cell 1998;94:161–170.
18. Fülöp V, Jones DT. Beta propellers: structural rigidity and functional diversity. Curr Opin Struct Biol 1999;9:715–721.
19. Paoli M. Protein folds propelled by diversity. Progress Biophys Mol Biol 2001;76:103–130.
20. Jawad Z, Paoli M. Novel sequences propel familiar folds. Structure (Camb) 2002;10:447–454.
21. Hiramatsu H, Kyono K, Higashiyama Y, Fukushima C, Shima H, Sugiyama S, Inaka K, Yamamoto A, Shimizu R. The structure and function of human dipeptidyl peptidase IV, possessing a unique eight-bladed beta-propeller fold. Biochem Biophys Res Commun 2003;302:849–854.
22. Engel M, Hoffmann T, Wagner L, Wermann M, Heiser U, Kiefersauer R, Huber R, Bode W, Demuth HU, Brandstetter H. The crystal structure of dipeptidyl peptidase IV (CD26) reveals its functional regulation and enzymatic mechanism. Proc Natl Acad Sci 2003;100:5063–5068.
23. Rasmussen HB, Branner S, Wiberg FC, Wagtmann N. Crystal structure of human dipeptidyl peptidase IV/CD26 in complex with a substrate analog. Nat Struct Biol 2003;10:19–25.
24. Szeltner Z, Rea D, Juhász T, Renner V, Fülöp V, Polgár L. Concerted structural changes in the peptidase and the propeller domains of prolyl oligopeptidase are required for substrate binding. J Mol Biol 2004;340:627–637.
25. Harris MN, Madura JD, Ming LJ, Harwood VJ. Kinetic and mechanistic studies of prolyl oligopeptidase from the hyperthermophile Pyrococcus furiosus. J Biol Chem 2001;276:19310–19317.
26. Jacobs DJ, Rader AJ, Kuhn LA, Thorpe MF. Protein flexibility predictions using graph theory. Proteins 2001;44:150–165.
27. Gohlke H, Kuhn LA, Case DA. Change in protein flexibility upon complex formation: analysis of Ras-Raf using molecular dynamics and a molecular framework approach. Proteins 2004;56:322–337.
28. Cornell WD, Cieplak P, Bayly CI, Gould IR, Merz KM Jr., Ferguson DM, Spellmeyer DC, Fox T, Caldwell JW, Kollman PA. A second generation force field for simulation of proteins, nucleic acids and organic molecules. J Am Chem Soc 1995;117:5179–5197.
29. Jorgensen WL, Chandrasekhar J, Madura J, Klein ML. Comparison of simple potential functions for simulating liquid water. J Chem Phys 1983;79:926–935.
30. Case DA, Pearlman DA, Caldwell JW, Cheatham III TE, Wang J, Ross WS, Simmerling CL, Darden TA, Merz KM, Stanton RV, and others. AMBER. 7. San Francisco: University of California; 2002.
31. Brooks BR, Janezic D, Karplus M. Harmonic analysis of large systems. I Methodology. J Comp Chem 1995;16:1522–1542.
32. van Aalten DM, Amadei A, Linssen AB, Eijsink VG, Vriend G, Berendsen HJ. The essential dynamics of thermolysin: confirmation of the hinge-bending motion and comparison of simulations in vacuum and water. Proteins 1995;22:45–54.
33. Amadei A, Linssen AB, Berendsen HJ. Essential dynamics of proteins. Proteins 1993;17:412–425.
34. Ichiye T, Karplus M. Collective motions in proteins: a covariance analysis of atomic fluctuations in molecular dynamics and normal mode simulations. Proteins 1991;11:205–217.
35. Szeltner Z, Renner V, Polgár L. Substrate- and pH-dependent contribution of oxyanion binding site to the catalysis of prolyl oligopeptidase, a paradigm of the serine oligopeptidase family. Protein Sci 2000;9:353–360.
36. Leatherbarrow RJ. GraFit. 5. UK: Erythacus Software Ltd., UK; 2001.
37. Cao ZW, Chen X, Chen YZ. Correlation between normal modes in the 20–200 cm^{-1} frequency range and localized torsion motions related to certain collective motions in proteins. J Mol Graph Model 2003;21:309–319.
38. Kleywegt GJ, Jones AT. Detection, delineation, measurement and display of cavities in macromolecular structures. Acta Crystallogr D Biol Crystallogr 1994;50:178–185.
39. Szeltner Z, Rea D, Renner V, Juliano L, Fülöp V, Polgár L. Electrostatic environment at the active site of prolyl oligopeptidase is highly influential during substrate binding. J Biol Chem 2003;278:48786–48793.
40. Polgár L, Patthy A. Cleavage of the Lys196-Ser197 bond of prolyl oligopeptidase: enhanced catalytic activity for one of the two active enzyme forms. Biochemistry 1992;31:10769–10773.
41. Polgár L. Unusual secondary specificity of prolyl oligopeptidase and the different reactivities of its two forms toward charged substrates. Biochemistry 1992;31:7729–7735.